

Transverse Momentum Dependent Factorization for Quarkonium Production at Low Transverse Momentum

J.P. Ma^{1,2}, J.X. Wang³ and S. Zhao¹

¹ *Institute of Theoretical Physics, Academia Sinica, P.O. Box 2735, Beijing 100190, China*

² *Center for High-Energy Physics, Peking University, Beijing 100871, China*

³ *Institute of High Energy Physics, Academia Sinica, P.O. Box 918(4), Beijing 100049, China*

Abstract

Quarkonium production in hadron collisions at low transverse momentum $q_{\perp} \ll M$ with M as the quarkonium mass can be used for probing transverse momentum dependent (TMD) gluon distributions. For this purpose, one needs to establish the TMD factorization for the process. We examine the factorization at the one-loop level for the production of η_c or η_b . The perturbative coefficient in the factorization is determined at one-loop accuracy. Comparing the factorization derived at tree level and that beyond the tree level, a soft factor is, in general, needed to completely cancel soft divergences. We have also discussed possible complications of TMD factorization of p-wave quarkonium production.

Quarkonium production in hadron collision can be used to explore the gluon content of hadrons, because the quarkonium is dominantly produced through gluon-gluon fusions. For the produced quarkonium with large transverse momentum, one can apply QCD collinear factorizations for long distance effects of the initial hadrons. In this case, one can extract the standard gluon distributions(see, e.g., [1]). If the quarkonium is produced with small transverse momentum q_{\perp} , it can be thought that the small q_{\perp} is generated at least partly from the transverse motion of gluons inside the initial hadrons. In this case, one can apply transverse momentum dependent(TMD) factorization for initial hadrons. Therefore, the production with small q_{\perp} allows access to TMD gluon distributions.

Factorizations with TMD quark distributions and fragmentation functions have been studied intensively beyond tree level in different processes in [2, 3, 4, 5]. In comparison, the factorization with TMD gluon distributions beyond tree level has only been studied for Higgs production in hadron collision in [6]. Recently, the TMD factorization of quarkonium production has been derived at tree level in [7], and based on it numerical predictions have been obtained. For theoretical consistency and precision, it is important to examine the TMD factorization beyond tree level. From early studies in [2, 3, 4, 6], it is known that a soft factor needs to be implemented into the factorization. In this work, we examine TMD factorization of η_c or η_b production at one-loop level.

A quarkonium is dominantly a bound state of a heavy quark Q and its antiquark \bar{Q} . Because of the heavy mass the $Q\bar{Q}$ pair is of a nonrelativistic system. To separate the nonperturbative effects related to the quarkonium in its production, one can employ nonrelativistic QCD (NRQCD) factorization [8] by an expansion of the small velocity of Q relative to \bar{Q} . The inclusive production of a quarkonium at moderate or large q_{\perp} has been studied intensively both in theory and in experiments. In the last five years, important progresses were made in the study of the next-to-leading order QCD correction for J/ψ production in hadron collisions [9] and power corrections [10]. The activities in this field can be seen in

[11]. It should be noted that in experiment it is also possible to study the inclusive production at low q_\perp . For example, a J/ψ produced at LHCb can be measured with q_\perp smaller than 1 GeV [12]. Therefore, with theoretically established TMD factorization, one can extract from experimental results TMD gluon distributions.

We will use the light-cone coordinate system, in which a vector a^μ is expressed as $a^\mu = (a^+, a^-, \vec{a}_\perp) = ((a^0 + a^3)/\sqrt{2}, (a^0 - a^3)/\sqrt{2}, a^1, a^2)$ and $a_\perp^2 = (a^1)^2 + (a^2)^2$. We introduce two light cone vectors $n^\mu = (0, 1, 0, 0)$ and $l^\mu = (1, 0, 0, 0)$ and the transverse metric $g_\perp^{\mu\nu} = g^{\mu\nu} - n^\mu l^\nu - n^\nu l^\mu$. We consider the process

$$h_A(P_A) + h_B(P_B) \rightarrow \eta_Q(q) + X, \quad (1)$$

in the kinematical region $Q^2 = q^2 \gg q_\perp^2$ with $Q = M_{\eta_Q}$ as the mass of η_Q , where η_Q stands for η_c or η_b . The momenta of the initial hadrons and of the quarkonium are given by

$$P_A^\mu \approx (P_A^+, 0, 0, 0), \quad P_B^\mu \approx (0, P_B^-, 0, 0), \quad q^\mu = (xP_A^+, yP_B^-, \vec{q}_\perp), \quad (2)$$

where we have neglected masses of hadrons, i.e., $P_A^- \approx 0$ and $P_B^+ \approx 0$. In the kinematic region of $q_\perp \ll Q$ TMD factorization can be applied with corrections suppressed by positive powers of q_\perp/Q . It is clear that in the kinematical region with $q_\perp \sim Q$ or $q_\perp \gg Q$ the TMD factorization can not be used. In these regions one can use collinear factorization as studied in [9].

For each hadron in the initial state, one can define its TMD gluon distribution. We introduce the gauge link along the direction $u^\mu = (u^+, u^-, 0, 0)$,

$$\mathcal{L}_u(z, -\infty) = P \exp \left(-ig_s \int_{-\infty}^0 d\lambda u \cdot G(\lambda u + z) \right), \quad (3)$$

where the gluon field is in the adjoint representation. At leading twist, one can define two TMD gluon distributions through the gluon density matrix [13],

$$\begin{aligned} & \frac{1}{xP^+} \int \frac{d\xi^- d^2\xi_\perp}{(2\pi)^3} e^{-ix\xi^- P_A^+ + i\vec{\xi}_\perp \cdot \vec{k}_\perp} \langle h_A | (G^{+\mu}(\xi) \mathcal{L}_u(\xi, -\infty))^a \left(\mathcal{L}_u^\dagger(0, -\infty) G^{+\nu}(0) \right)^a | h_A \rangle \\ & = -\frac{1}{2} g_\perp^{\mu\nu} f_{g/A}(x, k_\perp, \zeta_u^2, \mu) + \left(k_\perp^\mu k_\perp^\nu + \frac{1}{2} g_\perp^{\mu\nu} k_\perp^2 \right) h_{g/A}(x, k_\perp, \zeta_u^2, \mu), \end{aligned} \quad (4)$$

with $\xi^\mu = (0, \xi^-, \vec{\xi}_\perp)$. x is the momentum fraction carried by the gluon inside h_A . The gluon has also a nonzero transverse momentum \vec{k}_\perp . The definition is given in nonsingular gauges. It is gauge invariant. In singular gauges, one needs to add gauge links along transverse direction at $\xi^- = -\infty$ [14]. Due to the gauge links, the TMD gluon distributions also depend on the vector u through the variable

$$\zeta_u^2 = \frac{(2u \cdot P_A)^2}{u^2} \approx \frac{2u^-}{u^+} (P_A^+)^2. \quad (5)$$

In the definition, the limit $u^+ \ll u^-$ is taken in the sense that one neglects all contributions suppressed by negative powers of ζ_u^2 .

From the definition in Eq. (4), there are two TMD gluon distributions. The distribution $f_{g/A}$ corresponds to the standard gluon distribution in collinear factorization. The distribution $h_{g/A}$ describes gluons with linear polarization inside h_A . The relevant phenomenology of $h_{g/A}$ has been only recently studied [15, 16, 17]. Through the process studied here, one can also obtain information about this distribution [7]. For h_B , one can also define two TMD gluon distributions $f_{g/B}$ and $h_{g/B}$ similar to those in Eq. (4), in which the gauge links are along the direction $v^\mu = (v^+, v^-, 0, 0)$ instead of u and the limit

$v^+ \gg v^-$ is taken. Therefore, the two distributions $f_{g/B}$ and $h_{g/B}$ depend on the parameter ζ_v which is defined by replacing in ζ_u P_A with P_B and u with v in Eq. (5).

To study the TMD factorization of the process in Eq. (1), we need to study

$$g(p) + g(\bar{p}) \rightarrow \eta_Q(q) + X, \quad (6)$$

with $p^\mu = (P_A^+, 0, 0, 0)$ and $\bar{p}^\mu = (0, P_B^-, 0, 0)$. Since we are interested in the kinematical region of the small transverse momentum, we need to study the process in the limit of $q_\perp \ll Q = M_{\eta_Q}$. In reality, initial hadrons are bound states of partons. One can imagine that η_Q can be produced through two-gluon fusion, as in Eq. (6), in which one gluon is from the hadron h_A and another is from the hadron h_B . Certainly, there can be interactions or gluon exchanges between spectators in h_A and those in h_B and between partons involved in Eq. (6) and spectators. If these interactions are of short distances or if the exchanged gluons are hard, their effects in cross sections can be factorized with operators of higher twists because that the involved processes are a scattering of multipartons. These effects are power suppressed and can be neglected. A factorization may not be obtained if the interactions are of long distance or if the exchanged gluons are soft. It has been shown in Drell-Yan processes [3, 18] that the effects of soft-gluon exchanges are canceled or power suppressed if the sum of the unobserved states is completed. The exchanged gluons can be those collinear to the initial hadron h_A or h_B ; the effects of these collinear gluons can be factorized into the gauge links in the corresponding parton distribution functions. Since the process in Eq. (1) is similar to Drell-Yan processes, we expect that the conclusion made in [3, 18] for Drell-Yan processes also applies here. In our case, we have an observed η_Q in the final state. In general, η_Q is a bound state of a heavy-quark pair and possible light partons. We will use NRQCD for η_Q . In the approximation explained later, η_Q is effectively taken as a $Q\bar{Q}$ state in which the state is in color singlet and there is no relative momentum between Q and \bar{Q} . This $Q\bar{Q}$ is effectively pointlike and cannot emit soft gluons. Hence, there are no soft interactions between η_Q and spectators at leading power. With the arguments given in the above, we only need to study the process in Eq. (6) for factorization.

The reason why we only need to study the process in Eq. (6) at the leading power for the factorization can be understood in another way: If the factorization holds or is proven, it holds for arbitrary hadrons in the initial state. Especially, it also holds if the initial states are of partons. In the case with a factorization which is not rigorously proven, one can use parton states to study or to examine it, and to eventually prove it. In this work, we use the process in Eq. (6) to study the relevant factorization beyond tree level.

For long-distance effects related to η_Q , we use NRQCD factorization. We will work at the leading order of the small velocity expansion in NRQCD. At this order, the production of η_Q can be thought as a two-step process. In the first step, a $Q\bar{Q}$ pair is produced in which the heavy quark Q and its antiquark \bar{Q} carry the same momentum $q/2$. The pair is in color-singlet and spin-singlet 1S_0 . Then, the pair is transmitted into η_Q with the mass $Q = 2m_Q = M_{\eta_Q}$. The transition is described by a NRQCD matrix element. It is noted that the considered $Q\bar{Q}$ pair is in color singlet and hence there is no interaction of long distance between the $Q\bar{Q}$ pair and spectators of initial hadrons, as discussed before. At higher orders of the small velocity expansion the $Q\bar{Q}$ pair can be in the color-octet state [8]. With the color-octet $Q\bar{Q}$ pair it is possible that the NRQCD factorization proposed in [8] is violated beyond the one-loop level indicated by the study in [19].

At tree level, the process in Eq. (6) is with X as nothing. It is straightforward to obtain the differential cross section,

$$\begin{aligned} \frac{d\sigma}{dx dy d^2q_\perp} &= \sigma_0 \frac{\pi}{Q^2} \delta(xys - Q^2) \delta(1-x) \delta(1-y) \delta^2(\vec{q}_\perp), \\ \sigma_0 &= \frac{(4\pi\alpha_s)^2}{N_c(N_c^2 - 1)m_Q} |\psi(0)|^2, \end{aligned} \quad (7)$$

with $s = 2p^+\bar{p}^-$ and m_Q being the pole mass of the heavy quark. $\psi(0)$ is the wave function of η_Q at the origin. In fact, $|\psi(0)|^2$ should be expressed as a NRQCD matrix element. Beyond tree level, Coulomb singularities representing long-distance effects related to η_Q appear. These singularities are factorized into the NRQCD matrix element. At tree level, one easily finds

$$f_{g/A}^{(0)}(x, k_\perp, \zeta_u^2, \mu) = f_{g/B}^{(0)}(x, k_\perp, \zeta_v^2, \mu) = \delta(1-x)\delta^2(\vec{k}_\perp), \quad (8)$$

while $h_{g/A}$ and $h_{g/B}$ are zero. They become nonzero at order of α_s . With these results, one can write the tree-level cross section as a factorized form

$$\begin{aligned} \frac{d\sigma}{dx dy d^2q_\perp} &= \frac{\pi\sigma_0}{Q^2} \int d^2k_{a\perp} d^2k_{b\perp} f_{g/A}(x, k_{a\perp}) f_{g/B}(y, k_{b\perp}) \delta^2(\vec{k}_{a\perp} + \vec{k}_{b\perp} - \vec{q}_\perp) \delta(xys - Q^2) \mathcal{H}, \\ \mathcal{H} &= 1 + \mathcal{O}(\alpha_s). \end{aligned} \quad (9)$$

Beyond the tree level, one needs to introduce a soft factor. As we will see explicitly, all soft divergences will be factorized into the soft factor and TMD gluon distributions so that the perturbative coefficient \mathcal{H} is free from soft divergence. We will then determine \mathcal{H} at one-loop level.

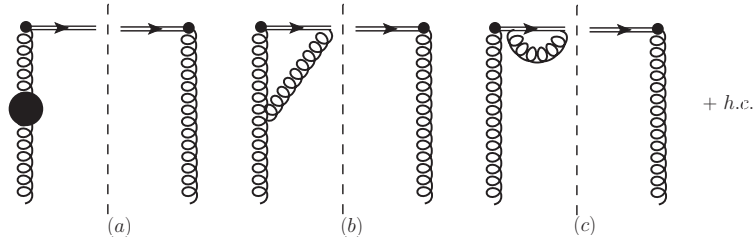


Figure 1: The one-loop corrections to the gluon TMD. The double lines represent the gauge link. The black bubble in Fig. 1a is for self-energy correction.

To derive the factorization at one loop, we need to study the one-loop corrections to TMD gluon distributions and the differential cross section. The one-loop correction to TMD gluon distribution has been studied in [6], where the collinear divergence has been regularized with an infinitely small off-shellness of the gluon. Here, we regularize all divergences in $d = 4 - \epsilon$ space-time. The correction can be divided into the virtual and real corrections. The virtual correction is given by diagrams in Fig. 1. We will use the $\overline{\text{MS}}$ scheme to subtract ultraviolet (UV) divergences. After the subtraction, we have the virtual correction from Fig. 1,

$$\begin{aligned} f_{g/A}^{(1)}(x, k_\perp, \zeta_u, \mu) \Big|_{vir.} &= \frac{\alpha_s}{4\pi} \delta(1-x) \delta^2(\vec{k}_\perp) \left[\left(-\frac{2}{\epsilon_s} + \ln \frac{e^\gamma \mu^2}{4\pi \mu_s^2} \right) \left(\frac{11}{3} N_c - \frac{2}{3} N_F \right) \right. \\ &\quad + 2N_c \left(-\frac{4}{\epsilon_s^2} - \frac{2}{\epsilon_s} \ln \frac{4\pi \mu_s^2}{e^\gamma \zeta_u^2} - \frac{1}{2} \ln^2 \frac{4\pi \mu_s^2}{e^\gamma \zeta_u^2} - \frac{5\pi^2}{12} + \left(-\frac{2}{\epsilon_s} + \ln \frac{e^\gamma \zeta_u^2}{4\pi \mu_s^2} \right) \right. \\ &\quad \left. \left. + \frac{1}{2} \ln \frac{\mu^2}{\zeta_u^2} - \frac{3}{2} \right) \right], \end{aligned} \quad (10)$$

where the poles in $\epsilon_s = 4 - d$ stand for collinear or infrared divergences, i.e., soft divergences. μ_s is the scale associated with these poles. μ is the UV scale. The terms in the first line in Eq. (10) is the sum

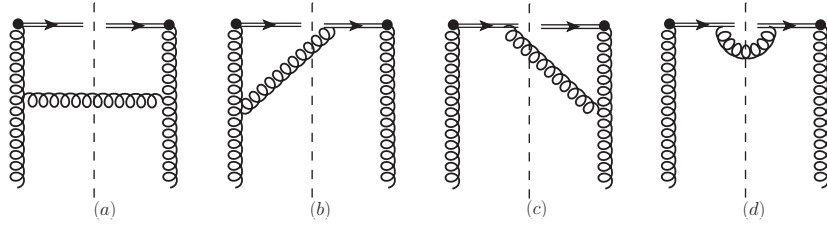


Figure 2: The real correction at one loop to the gluon TMD. The double lines represent the gauge link. These diagrams are for real corrections.

of the contributions from Fig. 1a and Fig. 1c with their conjugated diagrams. The remaining terms are from Fig. 1b and its conjugated diagram.

The corrections from Fig. 2 are real corrections. They can be found in [6] as

$$f_{g/A}^{(1)}(x, k_{\perp}, \zeta_u, \mu) \Big|_{re.} = \frac{\alpha_s N_c}{\pi^2 k_{\perp}^2} \left[\left(\frac{1-x}{x} + x(1-x) + \frac{x}{2} \right) - \frac{1}{2} \delta(1-x) \right. \\ \left. + \frac{x}{(1-x)_+} - \frac{x}{2} + \frac{1}{2} \delta(1-x) \ln \frac{\zeta_u^2}{k_{\perp}^2} \right], \quad (11)$$

where the terms in the first line are from Fig. 2a and Fig. 2d. The total one-loop correction is then the sum of the virtual and real corrections. At one loop, $h_{g/A}$ becomes nonzero. It receives a contribution from Fig. 2a. We have

$$h_{g/A}(x, k_{\perp}, \zeta_u, \mu) = \frac{2\alpha_s N_c}{\pi^2 (k_{\perp}^2)^2} \frac{1-x}{x} + \mathcal{O}(\alpha_s^2). \quad (12)$$

By replacing ζ_u with ζ_v we obtain $f_{g/B}$ and $h_{g/B}$ from $f_{g/A}$ and $h_{g/A}$, respectively.

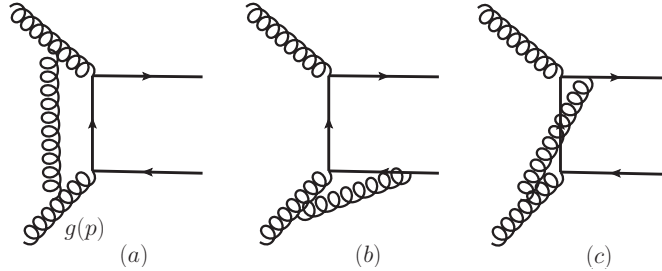


Figure 3: The class of diagrams where a gluon is emitted from the initial gluon $g(p)$ and is attached to a possible place. There are six diagrams. Three of them are given here. Another three diagrams are obtained by reversing the direction of the heavy quark line.

Now we turn to one-loop corrections of the differential cross section. The corrections can be divided into the virtual correction and the real correction. The virtual correction is the one-loop correction to the process $g(p) + g(\bar{p}) \rightarrow \eta_Q(q)$. We denote the total contribution from the virtual correction as

$$\frac{d\sigma(gg \rightarrow \eta_Q)}{dx dy d^2 q_{\perp}} \Big|_{vir.} = \frac{1}{2s(2\pi)^3} \delta(xys - Q^2) \delta(1-x) \delta(1-y) \delta^2(\vec{q}_{\perp}) \sigma_1. \quad (13)$$

The contributions to σ_1 can be divided into four parts,

$$\sigma_1 = \sigma_{1A} + \sigma_{1B} + \sigma_{1C} + \sigma_{1D}, \quad (14)$$

σ_{1A} receives contributions from diagrams in which a virtual gluon is emitted by the initial gluon $g(p)$. The diagrams for this part are given in Fig. 3. σ_{1B} receives contributions from diagrams in which a virtual gluon is emitted by the initial gluon $g(\bar{p})$. σ_{1C} denotes the contributions from diagrams in which a virtual gluon is exchanged between heavy quark line. σ_{1D} denotes the one-loop corrections of external gluon lines. This part will not contribute to \mathcal{H} , because the contributions to σ_{1D} are automatically subtracted into TMD gluon distributions. Below, we will only give and discuss the results of $\sigma_{1A,1B,1C}$.

In the above classification, Fig. 3a can contribute both to σ_{1A} and σ_{1B} . We put the half of the contribution Fig. 3a into σ_{1A} and another half into σ_{1B} . With symmetry arguments one easily finds $\sigma_{1A} = \sigma_{1B}$. We have then

$$\sigma_{1A} = \sigma_{1B} = \frac{1}{2}\sigma_1\Big|_{3a} + \sigma_1\Big|_{3b} + \sigma_1\Big|_{3c}. \quad (15)$$

By summing contributions from each diagram we obtain the following results for the virtual corrections:

$$\begin{aligned} \frac{\sigma_{1A}}{\sigma_0} &= \frac{\alpha_s N_c}{12\pi} \left[-6 \frac{4}{\epsilon_s^2} - 6 \frac{2}{\epsilon_s} \left(1 + \ln \frac{e^{-\gamma} 4\pi \mu_s^2}{Q^2} \right) - 3 \ln^2 \frac{e^{-\gamma} 4\pi \mu_s^2}{Q^2} - 6 \ln \frac{e^{-\gamma} 4\pi \mu_s^2}{Q^2} \right. \\ &\quad \left. + 9 \ln \frac{\mu^2}{Q^2} - 6 \ln 2 + 6 + \frac{11}{4} \pi^2 \right], \\ \frac{\sigma_{1C}}{\sigma_0} &= \frac{\alpha_s}{2\pi} \left[-N_c \ln \frac{\mu^2}{Q^2} + C_F \left(-2 + 4 \ln 2 \right) + \frac{1}{N_c} \left(2 \ln 2 - \frac{1}{4} \pi^2 \right) \right]. \end{aligned} \quad (16)$$

In these results, the UV poles are subtracted in the $\overline{\text{MS}}$ scheme. The on-shell scheme for the renormalization of heavy quark propagators is used so that $m_Q = Q/2$ is the pole mass of heavy quark. In σ_{1A} , the pole terms of ϵ_s are for soft divergences coming only from Fig. 3a. The contributions from Fig. 3b and Fig. 3c also contain collinear divergences and infrared divergences. The infrared divergences are canceled in the sum of the two diagrams, because the $Q\bar{Q}$ is in color singlet. The collinear divergences are also canceled. In calculating the diagrams for σ_{1C} one will meet Coulomb singularity. This singularity is factorized into NRQCD matrix element. Hence, we have finite σ_{1C} .

The real correction is from the tree-level process

$$g(p) + g(\bar{p}) \rightarrow \eta_Q(q) + g(k). \quad (17)$$

For the color-single $Q\bar{Q}$ pair, there are 12 diagrams for the amplitude. Since we are interested in the low q_\perp region, we expand the differential cross section in q_\perp/Q and only take the leading order in the expansion. At the leading order, we have only those diagrams given in Fig. 4 for the differential cross section. The result for the process in Eq. (17) in the limit of $q_\perp \rightarrow 0$ is

$$\begin{aligned} \frac{d\sigma}{dx dy d^2 q_\perp} &= \frac{\pi \sigma_0}{Q^2} \frac{N_c \alpha_s}{4\pi^2 q_\perp^2} \delta(xys - Q^2) \left[\frac{2\delta(1-y)}{x} \left(2 - 2x + 3x^2 - 2x^3 \right) + \frac{x(1+x)}{(1-x)_+} \delta(1-y) \right. \\ &\quad \left. - \delta(1-x)\delta(1-y) \ln \frac{q_\perp^2}{Q^2} + (x \leftrightarrow y) \right] + \mathcal{O}(q_\perp^0). \end{aligned} \quad (18)$$

The factorized result in Eq. (9) is derived at tree level. If we extend the factorization beyond tree level, with the one-loop results, in the above we will find the following: (i) The soft divergences are not

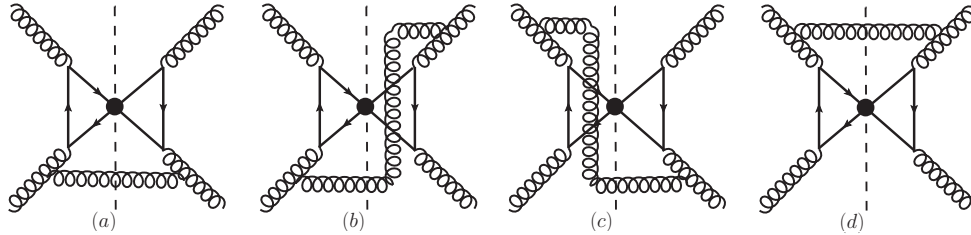


Figure 4: The diagrams for the cross section of $g + g \rightarrow g + \eta_Q$. In these diagrams, the gluon in the intermediate state is emitted or absorbed by gluons. The black dots denote the projection of the $Q\bar{Q}$ pair into the color singlet 1S_0 state. By reversing the quark lines, one can obtain other three diagrams from each diagram.

factorized, i.e., \mathcal{H} will contain some infrared divergences represented by poles in ϵ_s . (ii) The real correction of the differential cross section is not totally generated by TMD gluon distributions. In other words, \mathcal{H} will receive correction from the real correction. It results in that \mathcal{H} depends on q_\perp . All of these have a common reason. In the one-loop corrections to the differential cross section, there is an exchange of a soft gluon between the two initial gluons $g(p)$ and $g(\bar{p})$. In the virtual correction, the exchange results in infrared divergences, and in the real correction it results in contributions proportional to $\delta(1-x)\delta(1-y)$. The effects of the soft gluon exchange are not exactly generated by the corresponding soft gluon exchange in TMD gluon distributions. The effects of soft gluon exchange are of long distance. Therefore, one needs to introduce a soft factor in the factorization to completely factorize these effects from \mathcal{H} determined with Eq. (9).

The effects of soft gluon exchange between a gluon moving in the $+$ direction and a gluon moving in the $-$ direction can be described by the expectation value of a product with four gauge links. We introduce, as in [6],

$$S(\vec{b}_\perp, \mu, \rho) = \frac{1}{N_c^2 - 1} \langle 0 | \text{Tr} \left[\mathcal{L}_v^\dagger(\vec{b}_\perp, -\infty) \mathcal{L}_u(\vec{b}_\perp, -\infty) \mathcal{L}_u^\dagger(\vec{0}, -\infty) \mathcal{L}_v(\vec{0}, -\infty) \right] | 0 \rangle. \quad (19)$$

The gauge links are past pointing. It reflects the fact that the two gluons $g(p)$ and $g(\bar{p})$ are in the initial state. The dependence on the directions of gauge links is only through the parameter $\rho^2 = (2u \cdot v)^2 / (u^2 v^2) \approx u^- v^+ / (u^+ v^-)$. The limits $u^- \gg u^+$ and $v^+ \gg v^-$ are taken similarly to that in TMD gluon distributions. The gauge links or the gauge field is in the adjoint representation. At leading order, one has

$$S^{(0)}(\vec{b}_\perp, \mu, \rho) = 1. \quad (20)$$

At one loop, there are corrections from Fig. 5. One can divide the corrections into a virtual and a real part. The diagrams in the first row are of the virtual part. Those in the second row are of the real part. The virtual correction reads

$$S_{vir.}^{(1)}(\vec{b}_\perp, \mu, \rho) = \frac{\alpha_s N_c}{2\pi} \left[-\frac{2}{\epsilon_s} + \ln \frac{e^\gamma \mu^2}{4\pi \mu_s^2} \right] (2 - \ln \rho^2), \quad (21)$$

where the UV pole is subtracted. The pole in ϵ_s represents the IR divergence with the scale μ_s . The real part is

$$S_{re.}^{(1)}(\vec{b}_\perp, \mu, \rho) = -\frac{\alpha_s N_c}{2\pi^2} (2 - \ln \rho^2) \int d^2 k_\perp \frac{e^{-i\vec{b}_\perp \cdot \vec{k}_\perp}}{k_\perp^2}. \quad (22)$$

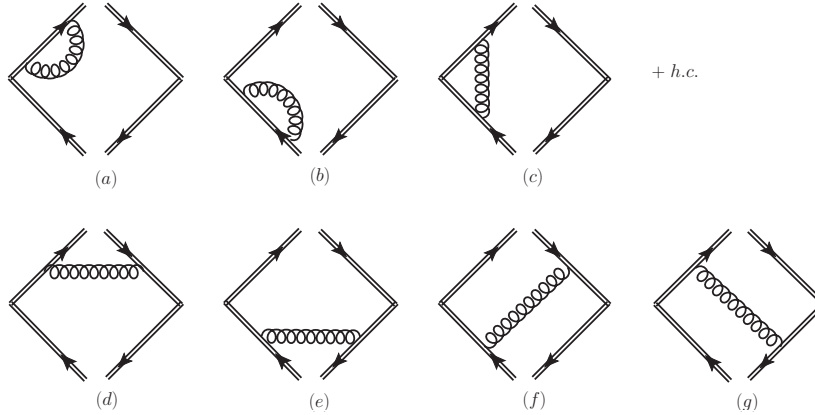


Figure 5: One-loop corrections for the soft factor. The first three diagrams plus their complex conjugated are virtual corrections. The last four diagrams are real corrections. A cut line is implied.

The total one-loop contribution is the sum of the virtual and real contributions.

We now define our soft factor which will enter the TMD factorization as

$$\begin{aligned}
\tilde{S}(\vec{\ell}_\perp, \mu, \rho) &= \int \frac{d^2 b_\perp}{(2\pi)^2} e^{i\vec{b}_\perp \cdot \vec{\ell}_\perp} S^{-1}(\vec{b}_\perp, \mu, \rho) \\
&= \delta^2(\vec{\ell}_\perp) - \frac{\alpha_s N_c}{2\pi} (2 - \ln \rho^2) \left[\left(-\frac{2}{\epsilon_s} + \ln \frac{e^\gamma \mu^2}{4\pi \mu_s^2} \right) \delta^2(\vec{\ell}_\perp) - \frac{1}{\pi \ell_\perp^2} \right] + \mathcal{O}(\alpha_s^2). \quad (23)
\end{aligned}$$

With the introduced soft factor, we propose the TMD factorization as

$$\begin{aligned}
\frac{d\sigma}{dx dy d^2 q_\perp} &= \frac{\pi \sigma_0}{Q^2} \int d^2 k_{a\perp} d^2 k_{b\perp} d^2 \vec{\ell}_\perp \delta^2(\vec{k}_{a\perp} + \vec{k}_{b\perp} + \vec{\ell}_\perp - \vec{q}_\perp) \delta(xys - Q^2) \\
&\quad \cdot f_{g/A}(x, k_{a\perp}, \zeta_u, \mu) f_{g/B}(y, k_{b\perp}, \zeta_v, \mu) \tilde{S}(\ell_\perp, \mu, \rho) \mathcal{H}(Q, \mu, \zeta_u, \zeta_v). \quad (24)
\end{aligned}$$

From one-loop results of the differential cross section, TMD gluon distributions, and the soft factor, we derive

$$\begin{aligned}
\mathcal{H}(Q, \mu, \zeta_u, \zeta_v) &= 1 + \frac{\alpha_s N_c}{4\pi} \left[\ln^2 \frac{\zeta_u^2}{Q^2} + \ln^2 \frac{\zeta_v^2}{Q^2} - \ln \rho^2 \left(1 + 2 \ln \frac{\mu^2}{Q^2} \right) + 2 \ln \frac{\mu^2}{Q^2} + \frac{7}{2} \pi^2 \right. \\
&\quad \left. + \frac{2}{N_c^2} \left(1 - \frac{1}{4} \pi^2 \right) \right] + \mathcal{O}(\alpha_s^2). \quad (25)
\end{aligned}$$

It is clear that \mathcal{H} is free from any soft divergence and does not depend on q_\perp . With the factorization the small transverse momentum, q_\perp is generated by the transverse motion of gluons in the initial hadrons and by soft gluon radiation. Equations (24) and (25) are our main results. It should be noted that the factorization holds for arbitrary large ζ_u and ζ_v . For practical applications, one may take a frame to simplify the results in Eqs. (24) and (25). One can take $\zeta_u^2 = \zeta_v^2 = \rho Q^2$ so that the TMD gluon distributions in Eq. (24) depend on ρ and Q^2 and the perturbative coefficient becomes a function of Q , μ , and ρ ,

$$\mathcal{H}(Q, \mu, \rho) = 1 + \frac{\alpha_s N_c}{2\pi} \left[\ln^2 \rho - \ln \rho \left(1 + 2 \ln \frac{\mu^2}{Q^2} \right) + \ln \frac{\mu^2}{Q^2} + \frac{7}{4} \pi^2 + \frac{1}{N_c^2} \left(1 - \frac{1}{4} \pi^2 \right) \right] + \mathcal{O}(\alpha_s^2). \quad (26)$$

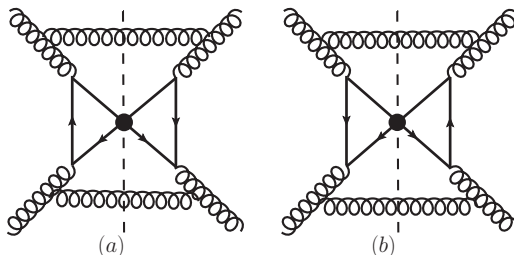


Figure 6: The diagrams for the cross section of $g + g \rightarrow g + g + \eta_Q$ give the contributions factorized with the gluon TMD g_k . By reversing the quark lines, one can obtain other three diagrams from each diagram.

At the considered orders, we will not find the contributions which can be factorized with $h_{g/A}$ or $h_{g/B}$ defined in Eq. (4). However, there is a contribution involving these distributions of linearly polarized gluons in the TMD factorization. This contribution can be found at a higher order of α_s from diagrams given in Fig. 6. It is straightforward to calculate these diagrams in the limit $q_\perp \rightarrow 0$. We find that the contribution takes the factorized form

$$\frac{d\sigma}{dx dy d^2 q_\perp} \Big|_{Fig.6} = \frac{\pi\sigma_0}{Q^2} \delta(xys - Q^2) \int d^2 k_{a\perp} d^2 k_{b\perp} \delta^2(\vec{k}_{a\perp} + \vec{k}_{b\perp} - \vec{q}_\perp) \left[f_{g/A}(x, k_{a\perp}) \Big|_{2a} f_{g/B}(y, k_{b\perp}) \Big|_{2a} - \frac{1}{2} \left((\vec{k}_{a\perp} \cdot \vec{k}_{b\perp})^2 - \frac{1}{2} k_{a\perp}^2 k_{b\perp}^2 \right) h_{g/A}(x, k_{a\perp}) h_{g/B}(y, k_{b\perp}) \right]. \quad (27)$$

Our result in the last line has also been derived in [7] with a different method. The perturbative coefficient of the contribution in the last line is at order of α_s^0 . This contribution should be added to Eq. (24). In principle one can determine the perturbative coefficient of the contribution beyond the leading order of α_s following the same way as has been done for Eqs. (24) and (25). However, this will be very tedious because one needs to calculate the partonic process $g + g \rightarrow \eta_Q + X$ at the 3-loop level. We leave this for a future study.

In the factorized form of the differential cross section in Eq. (25), the TMD gluon distributions do not depend on processes, they only depend on hadrons. The perturbative coefficient \mathcal{H} does not depend on initial hadrons. The soft factor \tilde{S} defined in Eqs. (19) and (23) is a basic quantity of QCD, i.e., it depends neither on hadrons or on processes. It is noted that the same soft factor also appears in TMD factorization of Higgs production studied in [6]. This indicates that soft divergences in different processes or in a class of processes can be factorized into the same object. This implies that the soft factor is universal at certain level. In TMD factorization of Drell-Yan processes, one also needs a soft factor to take radiation of soft gluons to complete the factorization[3, 4]. The soft factor there is similar to that defined in Eqs. (19) and (23). The only difference is that they are defined in different $SU(3)$ representations.

The studied TMD factorization can be used for the region with $q_\perp \sim \Lambda_{QCD}$ for extracting TMD gluon distributions. However, its usage is not limited to this kinematic region, because the factorization holds, in general, in the region $q_\perp/Q \ll 1$. In the region $Q \gg q_\perp \gg \Lambda_{QCD}$, both TMD factorization and collinear factorization hold. In the collinear factorization, the perturbative coefficient functions in this region contain large log of q_\perp/Q . The results from TMD factorization can be used to resum these large logs. This leads to the well-known Collins-Soper-Sterman resummation [3]. Based on our result here, one can also derive the resummation in the case of quarkonium production, similarly to that derived in [6].

We, therefore, do not discuss the details about the resummation here. We note that such a resummation has been studied very recently in [20]. An early work about the resummation can be found in [21], where the formation of a quarkonium from a $Q\bar{Q}$ pair is described with a color evaporation model instead of NRQCD factorization.

At the orders we have considered, the production of a p-wave quarkonium is possible. However, the TMD factorization in this case can be complicated. According to the NRQCD factorization in [8], one needs to consider not only the contribution from the production of a color singlet p-wave $Q\bar{Q}$ pair, but also the contribution of a color-octet s-wave $Q\bar{Q}$ pair. The formation of a p-wave quarkonium from the color-singlet and the color-octet $Q\bar{Q}$ pair is at the same order in the small velocity expansion. In the case we studied here, we only need to consider the contribution from production of a color-singlet s-wave $Q\bar{Q}$ pair. At the leading power the pair decouples with soft gluons. However, in the case of p-wave quarkonia, the color-singlet p-wave and color-octet s-wave $Q\bar{Q}$ pair can emit soft gluons at leading power. To completely separate the effects of soft gluons, one may need a different soft factor than that introduced here. This is also the reason why we write our TMD factorization in Eq. (24) explicitly with the unsubtracted TMD gluon distributions and the soft factor. Another complication with p-wave quarkonia is that one needs a gauge link for the NRQCD matrix element of the contribution from the color-octet $Q\bar{Q}$ pair to establish NRQCD factorization beyond one loop, as shown in [19]. We will examine the TMD factorization for p-wave quarkonium in a separate publication.

Before summarizing our work, we note that one can define subtracted TMD gluon distributions as those used for Higgs production in [6], to factorize the differential cross section. Then, our result can be factorized as the same form in [6] only with the difference that the perturbative coefficient is different. One may also redefine TMD gluon distributions as suggested in [22] so that the differential cross section is factorized only with the redefined TMD gluon distributions. Due to this and the reason discussed for p-wave quarkonium, we only give our results factorized with the unsubtracted TMD gluon distributions as in Eq. (24).

To summarize, we have studied the one-loop TMD factorization of 1S_0 -quarkonium production in a hadron collision at low transverse momentum. We find that the differential cross section can be factorized with the TMD gluon distributions, the soft factor, and the perturbative coefficient. The TMD gluon distributions and the soft factor are consistently defined with QCD operators; the perturbative coefficient is determined here at one loop. In comparison with the factorization derived at tree level, the soft factor is needed to cancel all effects of soft gluons. Our result will be useful not only for extracting TMD gluon distributions from experimental data, but also for resumming large logs of q_\perp appearing in the collinear factorization.

Acknowledgments

We would like to thank Prof. Y.-N. Gao for a discussion about LHCb experiment and G. P. Zhang for discussions about TMD parton distributions. The work of J. P. M. is supported by National Nature Science Foundation of People's Republic of China (Grants No. 10975169, 11021092, and No. 11275244). The work of J. X. W. is supported by the National Natural Science Foundation of Peoples Republic of China (Grants No. 10979056 and No. 10935012), and in part by DFG and NSFC (CRC 110).

References

- [1] A. D. Martin, C.-K. Ng, and W. J. Stirling, Phys. Lett. B **191**, 200 (1987).
- [2] J. C. Collins and D. E. Soper, Nucl. Phys. **B193**, 381 (1981); Nucl. Phys. **B213**, 545(E) (1983); Nucl. Phys. **B197**, 446 (1982); Nucl. Phys. **B194**, 445 (1982).
- [3] J. C. Collins, D. E. Soper, and G. Sterman, Nucl. Phys. **B250**, 199 (1985).
- [4] X. D. Ji, J. P. Ma, and F. Yuan, Phys. Rev. D **71**, 034005 (2005); Phys. Lett. B **597**, 299 (2004).
- [5] J. C. Collins and A. Metz, Phys. Rev. Lett. **93**, 252001 (2004).
- [6] X. D. Ji, J. P. Ma, and F. Yuan, J. High Energy Phys. **07** (2005) 020.
- [7] D. Boer and C. Pisano, Phys. Rev. D **86**, 094007 (2012).
- [8] G. Bodwin, E. Braaten, and G. P. Lepage, Phys. Rev. D **51**, 1125 (1995); *ibid.* **55**, 5853(E) (1997).
- [9] J. Campbell, F. Maltoni, F. Tramontano, Phys. Rev. Lett. **98**, 252002 (2007); B. Gong and J.-X. Wang, Phys. Rev. Lett. **100**, 232001 (2008); B. Gong, X.-Q. Li, and J.-X. Wang, Phys. Lett. B **673**, 197 (2009); Y. Q. Ma, K. Wang, and K. T. Chao, Phys. Rev. Lett. **106**, 042002 (2011); Y. Q. Ma *et al.*, Phys. Rev. Lett. **108**, 242004 (2012); M. Butenschoen and B. A. Kniehl, Phys. Rev. Lett. **106**, 022003 (2011); Phys. Rev. Lett. **108**, 172002 (2012); B. Gong, L. P. Wan, J. X. Wang, and H. F. Zhang, Phys. Rev. Lett. **110**, 042002 (2013).
- [10] Z.-B. Kang, J.-W. Qiu, and G. Sterman, Phys. Rev. Lett. **108**, 102002 (2012); S. Fleming, A. K. Leibovich, T. Mehen, and I. Z. Rothstein, Phys. Rev. D **86**, 094012 (2012).
- [11] N. Brambilla *et al.*, Eur. Phys. J. C **71**, 1534 (2011).
- [12] R. Aaij *et al.*(LHCb Collaboration), Eur. Phys. J. C **71**, 1645 (2011).
- [13] P. J. Mulders and J. Rodrigues, Phys. Rev. D **63**, 094021 (2001).
- [14] X. D. Ji and F. Yuan, Phys. Lett. B **543**, 66 (2002); A. V. Belitsky, X. D. Ji, and F. Yuan, Nucl. Phys. **B656**, 165 (2003).
- [15] D. Boer, W. J. den Dunnen, C. Pisano, M. Schlegel, and W. Vogelsang, Phys. Rev. Lett. **108**, 032002 (2012).
- [16] F. Dominguez, J.-W. Qiu, B.-W. Xiao, and F. Yuan, Phys. Rev. D **85**, 045003 (2012), e-Print: arXiv:1109.6293 [hep-ph].
- [17] A. Metz and J. Zhou, Phys. Rev. D **84**, 051503 (2011).
- [18] J. C. Collins, D. E. Soper, and G. T. Sterman, Nucl. Phys. **B261**, 104 (1985).
- [19] G. C. Nayak, J.-W. Qiu, and G. F. Sterman, Phys. Lett. B **613**, 45 (2005), Phys. Rev. D **74**, 074007 (2006).
- [20] P. Sun, C.-P. Yuan, and F. Yuan, arXiv:1210.3432.

- [21] E. L. Berger, J.-W. Qiu, and Y.-L. Wang, Phys. Rev. D **71**, 034007 (2005).
- [22] J. Collins, *Foundations of perturbative QCD*, (Cambridge University Press, Cambridge, 2011); Int. J. Mod. Phys. Conf. Ser. **04**, 85 (2011).